Convex lattice polygons of fixed area with perimeter dependent weights

R. Rajesh[1] and Deepak Dhar[2]

[1]*Department of Physics - Theoretical Physics, University of Oxford, 1 Keble Road, Oxford OX1 3NP, UK*
[2]*Department of Theoretical Physics, Tata Institute of Fundamental Research, Homi Bhabha Road, Mumbai 400005, India*

(Dated: March 27, 2003)

We study fully convex polygons with a given area, and variable perimeter length on square and hexagonal lattices. We attach a weight t^m to a convex polygon of perimeter m and show that the sum of weights of all polygons with a fixed area s varies as $s^{-\theta_{conv}} e^{K\sqrt{s}}$ for large s and t less than a critical threshold t_c, where K is a t-dependent constant, and θ_{conv} is a critical exponent which does not change with t. We find θ_{conv} is $1/4$ for the square lattice, but $-1/4$ for the hexagonal lattice. The reason for this unexpected non-universality of θ_{conv} is traced to existence of sharp corners in the asymptotic shape of these polygons.

PACS numbers: 05.50.+q, 64.60.Ak
Keywords: convex polygons; percolation; directed percolation

I. INTRODUCTION

The study of polygons is an important problem in lattice statistics [1]. It has been studied in the context of self-avoiding walks, and as a model of the shape transition in vesicles [2, 3]. The problem is also related to the statistics of rare large clusters in percolation theory (see below). There has been considerable progress in counting exactly various sub-classes of polygons weighted by area and perimeter (see [4, 5] and references within). Recently, the exact critical scaling function of these polygons has also been found [6, 7, 8, 9].

Convex polygons are an important sub-class of polygons. They are defined as follows. The area enclosed by a polygon on a lattice is a simply connected set of elementary plaquettes or cells of the lattice. A polygon on a square lattice is said to be column-convex if all the plaquettes in any column are connected through plaquettes in the same column. The polygon is convex if it is column-convex in both the horizontal and vertical directions (see Fig. 1). A polygon on a hexagonal lattice is said to be convex if it is column-convex in all its three lattice directions (see Fig. 2).

Let $C_{m,s}$ be the number of convex polygons with perimeter m and area s. We define the generating function

$$C_s(t) = \sum_m C_{m,s} t^m. \tag{1}$$

For any finite s, this is a finite polynomial, and hence convergent. For large s, there exists a $t_c < 1$ such that for all $0 < t < t_c$, the leading contribution to the sum in Eq. (1) comes from polygons whose perimeter is of order $\sqrt{s}$. For the square lattice $t_c = 1/2$. It is straightforward to prove upper and lower bounds on this sum which vary as an exponential of $\sqrt{s}$. It is expected that the leading correction to the exponential behavior is a power law,

$$C_s(t) \sim s^{-\theta_{conv}} e^{K(t)\sqrt{s}},\ s \to \infty,\ t < t_c, \tag{2}$$

where $K(t)$ is a t-dependent function, and θ_{conv} is a critical exponent. When t tends to zero, $K(t)$ tends to $C\ln(t)$, where $C = 4$ for the square lattice. The power-law exponent θ corresponding to other sub-classes of polygons will be denoted by a suitable subscript.

In this paper, we calculate θ_{conv} for convex polygons on the square and hexagonal lattices by summing over all polygons with a fixed area and weighted by perimeter, and show that θ_{conv} for the square lattice is $1/4$, but for the hexagonal lattice it is $-1/4$. We explain this difference by showing that the asymptotic shape of large convex polygons on square and hexagonal lattices consist of 4 and 6 cusps respectively. For a polygon whose macroscopic shape shows n cusps, we argue that the value of θ is $(5-n)/4$.

In the percolation problem (see [10, 11] for an introduction) above the percolation threshold, the probability $\mathrm{Prob}_p(s)$ of finite clusters of size s in d-dimensions is expected to vary as [12, 13]

$$\mathrm{Prob}_p(s) \sim s^{-\theta_{perc}} \exp\left(-B(p) s^{\frac{d-1}{d}}\right), \quad s \to \infty. \tag{3}$$

Here the exponent θ_{perc} is expected to be universal, same for all p above the critical percolation threshold. For these rare large clusters in two dimensions, the linear size of a cluster of s sites varies as $\sqrt{s}$. It has a few holes, and the external boundary of the cluster has overhangs. These are normally expected to be irrelevant. On ignoring holes, we can model percolation clusters by hole-less clusters, and $\mathrm{Prob}_p(s)$ would have the same qualitative behavior. In particular, $\theta_{perc} = \theta_{poly}$, where θ_{poly} is the power-law exponent in Eq. (1) corresponding to all lattice polygons with a fixed area.

The macroscopic shape of rare large clusters for $p > p_c$ is convex. Local fluctuations of the surface at a non-zero angle to the x-axis can be well approximated by the fluctuations of a staircase path. As most of the surface of the cluster has a non-zero finite slope, one may expect that dominant contribution to $\mathrm{Prob}_p(s)$ comes from convex polygons. This would imply that $\theta_{perc} = \theta_{poly} = \theta_{conv}$. Our results show that both these equalities cannot be correct simultaneously. Presumably, the second equality is wrong as θ_{conv} turns out to be lattice dependent. For the

percolation problem, the presumably exact value of θ_{perc} has been calculated in all dimensions using techniques of continuum field theory, within the droplet model which ignores the holes and overhangs in the clusters [13]. In two dimensions $\theta_{perc} = 5/4$.

We now briefly review known results for convex polygons. For convex polygons on a square lattice, the exact two-variable generating function $C(t,z)$ defined as

$$C(t,z) = \sum_s C_s(t) z^s, \tag{4}$$

was calculated by Lin [14] and Bousquet-Mélou [15, 16]. It was shown that

$$C(t,z) = G + 2\sum_{m=2}^{\infty} g_m \sum_{n=1}^{m-1} t^{-2n} \sum_{p=0}^{\infty} f_{n+p} + \sum_{m=3}^{\infty} g_m S_m, \tag{5}$$

where

$$\begin{aligned}
g_m(t,z) &= t^{2m} \sum_{n=1}^{\infty} (t^2 z)^n \prod_{k=1}^{n} (1-z^k)^{-2} \left[u_{m-1,n} - (2+z^n)u_{m-2,n} + (1+2z^n)u_{m-3,n} - z^n u_{m-4,n}\right], \\
u_{k,n}(t,z) &= \sum_{r=0}^{k} \prod_{m=1}^{n+r} (1-z^k) \prod_{m=1}^{n+k-r} (1-z^k) \prod_{m=1}^{r} (1-z^k)^{-1} \prod_{m=1}^{k-r} (1-z^k)^{-1}, \quad k \geq 0, \\
G(t,z) &= \sum_{m=1}^{\infty} g_m(t,z), \\
S_m(t,z) &= \sum_{n=1}^{m-2} g_n t^{-2n} (m-n-1), \\
f_m(t,z) &= h_m + \sum_{n=2}^{m} S_{n+1} \left[\frac{t^2 z}{h_1' - h_1} \left(h_m (h_n' - h_m)\right) + \delta_{m,n} t^{2n+2} z^n\right], \\
h_n(t,z) &= t^{2n+2} z^n \left(1 + \sum_{m=1}^{\infty} \frac{(-t^2)^m z^{m(m+1+2n)/2}}{\prod_{r=1}^{m} (1-z^r)(1-t^2 z^r)}\right) \left(1 + \sum_{m=1}^{\infty} \frac{(-t^2)^m z^{m(m+1)/2}}{\prod_{r=1}^{m} (1-z^r)(1-t^2 z^r)}\right)^{-1}, \\
h_n'(t,z) &= t^2 z^n \left(1 + \sum_{m=1}^{\infty} \frac{(-t^2)^m z^{m(m+1+2n)/2}}{\prod_{r=1}^{m} (1-z^r)(t^2-z^r)}\right) \left(1 + \sum_{m=1}^{\infty} \frac{(-t^2)^m z^{m(m+1)/2}}{\prod_{r=1}^{m} (1-z^r)(t^2-z^r)}\right)^{-1}.
\end{aligned} \tag{6}$$

It is not easy to extract the asymptotic behavior of $C_s(t)$ for large s and fixed small value of t from the complicated expressions Eqs. (5) and (6).

The asymptotic behavior of the coefficient of t^m in Eq. (4), when $z > 1$, was determined in Ref. [17]. In this case, the dominant contribution comes from the largest s possible, which is $z^{m^2/16}$ [3]. To be more specific, it was proved [17] that for fixed $z > 1$

$$\sum_s C_{m,s} z^s = A(z) z^{m^2/16} (1 + (\rho^m)), \ m \to \infty, \tag{7}$$

for some $\rho < 1$. The function $A(z)$ was shown to behave as

$$A(z) \sim \frac{1}{4} \left(\frac{\epsilon}{2\pi}\right)^{3/2} e^{2\pi^2/(3\epsilon)} \text{ as } \epsilon = \ln(z) \to 0^+. \tag{8}$$

These results are valid when $\epsilon m \gg 1$. We are interested in the case when $\epsilon \to 0^-$ with $m \sim \sqrt{s} \sim 1/\epsilon$. It is not clear how to extend the results Eqs. (7) and (8) in this regime. However, if we *assume* that the results remain valid qualitatively in this regime also, and the limits of m large and ϵ small can be taken in reverse order, we can estimate $C_{s,t}$ by

$$C_s(t) = \sum_m t^m \frac{1}{2\pi i} \oint \frac{dz}{z^{s+1}} \sum_s C_{m,s} z^s. \tag{9}$$

Equation (9) can be evaluated by the method of steepest descent giving $C_s(t) \sim s^{-5/4} e^{\sqrt{s} K(t)}$. This conclusion seems to be correct for all polygons, but as we shall show later in the paper, it is incorrect for convex polygons. This implies that in the regime of interest, the asymptotic behavior is indeed different and not given by Eqs. (7) and (8).

The rest of the paper is organized is as follows. In Sec. II, the exponent θ_{conv} is calculated for the square and hexagonal lattice. In Sec. III, the macroscopic shape of convex polygons is determined. In Sec. IV, the results are extended to sub-classes of convex polygons. In Sec. V, the macroscopic shape of column-convex polygons is determined. Finally, we end with a summary and

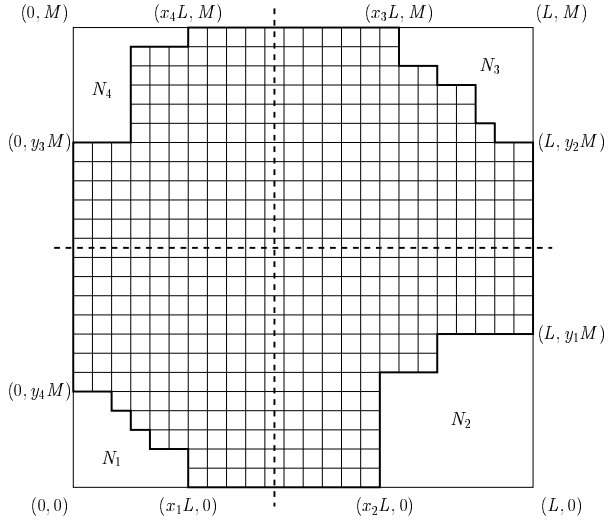

FIG. 1: A typical convex polygon on a square lattice and its bounding box is shown. All vertical and horizontal straight lines (dotted in the figure) intersect the polygon either 0 or 2 times. The convex polygon can be thought of as a rectangle from whose corners some squares have been removed by staircase like paths.

conclusions in Sec. VI.

II. CALCULATION OF THE EXPONENT θ_{conv}

Consider convex polygons on a square lattice. A convex polygon of a given perimeter can be visualized as a bounding rectangle of the same perimeter from each of whose four corners squares have been removed by staircase like paths (see Fig. 1). Such paths are also known as Ferrers diagrams in the combinatorics literature. These staircase paths have the constraint that they cannot intersect each other. All convex polygons may then be generated by considering all possible rectangles.

Let $R(z, A, B)$ be a generating function such that the coefficient of z^s enumerates the number of staircase paths from $(0, A)$ to $(B, 0)$ enclosing an area s. We then obtain

$$\sum_s C_s(t) z^s \sim \sum_{x_i, y_i, L, M} t^{2(L+M)} z^{LM} \times R(z^{-1}, x_1 L, y_4 M)\ R(z^{-1}, (1-x_3)L, (1-y_2)M) \times R(z^{-1}, (1-x_2)L, y_1 M)\ R(z^{-1}, x_4 L, (1-y_3)M), \quad (10)$$

where we refer to Fig. 1 for the notation. In writing down Eq. (10) we have ignored the case when the staircases at two opposite corners may intersect. This will only make an exponentially small correction and will not modify the exponent θ_{conv}. From the theory of partitions [18], it is known that

$$R(z, A, B) = z^{A+B-1} \frac{(z)_{A+B-2}}{(z)_{A-1}(z)_{B-1}}, \quad (11)$$

where

$$(z)_A = \prod_{k=1}^{A} (1 - z^k). \quad (12)$$

The asymptotic behavior of the coefficient of z^s in $R(z, A, B)$ for large s can be calculated by the method of steepest descent. To evaluate $(z)_A$, we take logarithms on both sides of Eq. (12) and convert the resultant sum into an integral by using the Euler-Maclaurin sum formula [19]. This gives

$$(z)_A \sim \frac{1}{\sqrt{\epsilon}} \exp\left(\frac{1}{\epsilon} \int_{e^{-\epsilon A}}^{1} \frac{\ln(1-x)}{x} \right), \quad \epsilon = -\ln(z) \to 0. \quad (13)$$

We would be interested in the limit when A and B vary as $\sqrt{s}$. Let $A = a\sqrt{s}$ and $B = b\sqrt{s}$. Then, the coefficient of z^s in $R(z, A, B)$ is given by

$$\frac{1}{2\pi i} \oint \frac{R(z, A, B)}{z^{s+1}} \sim \frac{1}{s^{3/4}} \int d\alpha e^{\sqrt{s} g(\alpha, a, b)}, \quad (14)$$

where we made the substitution $z = e^{-\alpha/\sqrt{s}}$, and the function $g(\alpha, a, b)$ is given by

$$g(\alpha, a, b) = \alpha + \frac{1}{\alpha} \Bigg(\int_{e^{-\alpha(a+b)}}^{1} du \frac{\ln(1-u)}{u} - \int_{e^{-\alpha a}}^{1} du \frac{\ln(1-u)}{u} - \int_{e^{-\alpha b}}^{1} du \frac{\ln(1-u)}{u} \Bigg). \quad (15)$$

The function $g(\alpha, a, b)$ has has a minimum at some $\alpha = \alpha_0$ where α_0 is a function of a and b. On doing the integral in Eq. (14) by the method of steepest descent, the power law factor gets modified by a factor $s^{-1/4}$. Thus, we obtain

$$\frac{1}{2\pi i} \oint \frac{R(z, A, B)}{z^{s+1}} \sim \frac{1}{s} \exp\left[\sqrt{s} f(A/\sqrt{s}, B/\sqrt{s}) \right], \quad (16)$$

where

$$f(a, b) = g(\alpha_0, a, b), \quad (17)$$

with $g(\alpha, a, b)$ as in Eq. (15) and α_0 being that value of α which minimizes $g(\alpha, a, b)$. The function $f(a, a)$ increases monotonically from 0 to $\pi\sqrt{2/3}$ when a increases from 1 to ∞. The value at infinity, $f(\infty, \infty)$, corresponds to the result for unrestricted partitions [20]. Clearly, the function $f(a, b)$ is a monotonically increasing function in both its variables.

From now onwards, we will consider the case when all the distances in Fig. 1 scales as $\sqrt{s}$, i.e., $L = l\sqrt{s}$, and $M = m\sqrt{s}$. Also, each of the N_i's varies linearly with s, i.e., $N_i = n_i s$. Equation (10) then reduces to

$$C_s(t) \sim \int \prod_{i=1}^{4} (dx_i dy_i dn_i) dl dm \left(\sqrt{s}\right)^{10} s^4 \delta\left[s\left(1+\sum n_i - lm)\right)\right] t^{2\sqrt{s}(l+m)}$$
$$\times \frac{1}{s^4} \exp\left(\sqrt{s}\left[\sqrt{n_1} f\left(\frac{x_1 l}{\sqrt{n_1}}, \frac{y_4 m}{\sqrt{n_1}}\right) + \sqrt{n_2} f\left(\frac{(1-x_2)l}{\sqrt{n_2}}, \frac{y_1 m}{\sqrt{n_2}}\right)\right]\right)$$
$$\times \exp\left(\sqrt{s}\left[\sqrt{n_3} f\left(\frac{(1-x_3)l}{\sqrt{n_3}}, \frac{(1-y_2)m}{\sqrt{n_3}}\right) + \sqrt{n_4} f\left(\frac{x_4 l}{\sqrt{n_4}}, \frac{(1-y_3)m}{\sqrt{n_4}}\right)\right]\right), \quad (18)$$

where the $(\sqrt{s}))^{10}$ factor is due to the scaling of the distances, the s^4 factor is due to scaling of the N_i's and s^{-4} factor is due to the power law term in the asymptotic formula for partitions. Thus, there is an overall power law factor s^5.

In the limit of large s, the integrals can be performed by the saddle point method. We first note that the shape that has maximum contribution to the integral will have the symmetry of the square lattice, i.e., the bounding box will be a square of side $x_0\sqrt{s}$ and each of the N_i's will be equal to $\beta_0 s$. Consider the integration over the variables x_2, y_2, x_3, y_3 about this shape. Due to the monotonic behavior of the scaling function $f(x, y)$, the integrand is maximum with respect to these four variables at the end points of their limits of integration, namely x_1, y_1, x_3, y_3 respectively. On doing the saddle point integration, the contribution to θ_{conv} in the power law prefactor from each integration is $s^{-1/2}$. Thus, we are left with a power law term s^3. With respect to the remaining coordinate variables x_1, y_1, x_3, y_3, l, m, the integrand takes on it maximum value at a point in the interior of the region of integration, and each such integration contributes a factor $s^{-1/4}$ to the power law prefactor. Thus, after integrating over all the coordinates, a power law factor of $s^{3/2}$ remains.

Now, only the integrals over the n_i's remain to be done. Out of the four integrals, one of them integrates away the delta function contributing a factor s^{-1}, while each of the others contributes a factor $s^{-1/4}$ to the power law prefactor. Collecting together these terms, we obtain

$$C_s(t) \sim \frac{1}{s^{1/4}} e^{4\sqrt{s}\left(\sqrt{\beta_0} f\left(\frac{x_0}{2\sqrt{\beta_0}}, \frac{x_0}{2\sqrt{\beta_0}}\right) + x_0 \ln(t)\right)}. \quad (19)$$

We compute the term in the exponential in Eq. (19) in Sec. III (see Eq. (28)). Equation (19) implies that for convex polygons on a square lattice

$$\theta_{conv}^{sq} = \frac{1}{4}. \quad (20)$$

The above calculation of θ_{conv} can be summarized as follows. Consider a convex polygon constructed from a bounding box by n staircase paths ($n = 4$ for square lattice). The end points of the staircase paths can slide along the bounding box, and each path contributes three coordinates to be integrated over. Out of these $3n$ coordinates, two of them are fixed to prevent over counting of polygons which are identical modulo translations. Thus, there are a total of $(3n-2)$ coordinates, each one of them varying as $\sqrt{s}$, to be integrated over. Each staircase path also encloses an area, varying as s, that has to be integrated over. Finally, there is a contribution s^{-1} from each such area, corresponding to the enumeration of staircase paths with fixed ends and fixed area. Thus, the integrand has an overall power law factor $s^{(3n-2)/2}$ to start with. On doing the integrations, the first n coordinate integrals contribute a factor $s^{-1/2}$ each as the maximum occurs at the end points of the integration limits, while the remaining $(2n-2)$ coordinates contribute $s^{-1/4}$ each. Thus, after the integration over the coordinates, the power law factor is $s^{(n-1)/2}$. The integrations over the areas have the following contributions. One of them integrates over the delta function, contributing s^{-1}, while each of the other contribute a factor $s^{-1/4}$. Taking these corrections into account, we obtain that θ_{conv} for a

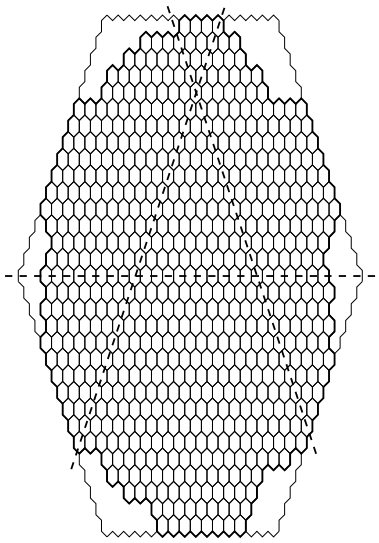

FIG. 2: A typical convex polygon on a hexagonal lattice is shown. Any straight line in the three lattice directions (shown as dotted lines) intersect the polygon at most twice. The convex polygon can be thought of 6 blocks carved out by directed staircase like paths from a bounding hexagon.

n-sided convex polygon is

$$\theta_{conv}^{n\text{-}sided} = \frac{5-n}{4}. \tag{21}$$

We recover the square lattice result (Eq. (20)) when $n = 4$ in Eq. (21)

Consider now convex polygons on a hexagonal lattice (see Fig. 2). It is quite straightforward to carry out a similar analysis as was done for the square lattice. Equivalently, putting $n = 6$ in the expression for θ_{conv} for n-sided convex polygons, we obtain

$$\theta_{conv}^{hex} = -\frac{1}{4}. \tag{22}$$

Equations (20) and (22) imply that θ_{conv} is not universal for convex polygons and takes on different values on different lattices.

III. MACROSCOPIC SHAPE OF CONVEX POLYGONS

The fact that θ_{conv} for the square and hexagonal lattices comes out different is somewhat unexpected. To understand the reason for this difference, and why this differs from the value $\theta_{perc} = 5/4$ for percolation clusters, we need to look at the macroscopic shape of convex polygons. This can be done exactly using the Wulff construction [21]. Consider the case on the square lattice. The equilibrium curve is the one that extremises the free energy functional

$$\mathcal{L}[y(x)] = \int_0^X dx\sigma(y')\sqrt{1+y'^2} - \frac{2\lambda}{\sqrt{s}}\int_0^X y dx, \tag{23}$$

where $y' = dy/dx$, $\sigma(y')$ is the orientation dependent surface tension and λ is a Lagrange multiplier. The equilibrium curve $y_0(x)$ satisfies the Euler-Lagrange equation

$$-\frac{d}{dx}\left(\frac{d}{dy'}\left(\sigma(y')\sqrt{1+y'^2}\right)\right) - \frac{2\lambda}{\sqrt{s}} = 0. \tag{24}$$

The equilibrium macroscopic shape is then obtained by minimizing $\mathcal{L}[y_0(x)]$ with respect to the endpoint X.

For convex polygons, it is easy to determine the slope dependent surface tension exactly. It has two contributions: one coming from the energy of the interface, and one from the entropy. For an interface having X horizontal and Y vertical steps, the energy per unit length is proportional to $|X| + |Y|$, and the number of configurations is $(|X| + |Y|)!/|X|!|Y|!$. This gives

$$\begin{aligned}\sigma(y')\sqrt{1+y'^2} \;=\; & -(1+|y'|)\ln(1+|y'|) + |y'|\ln(|y'|) \\ & -(1+|y'|)\ln(t).\end{aligned} \tag{25}$$

Following the above procedure, we obtain that the macroscopic shape of the staircase satisfies the equation

$$e^{-2\lambda|y|/\sqrt{s}} + e^{-2\lambda|x|/\sqrt{s}} = t^{-1}, \tag{26}$$

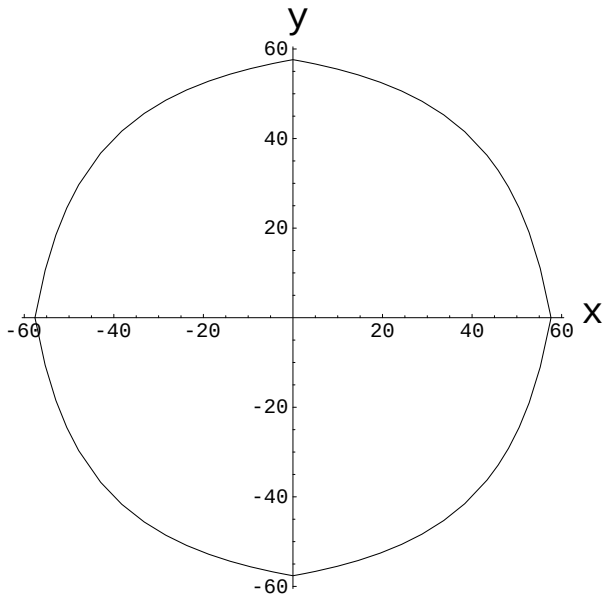

FIG. 3: The equilibrium shape of a convex polygon on a square lattice enclosing an area 10000 when the perimeter weight $t = 0.15$ is shown.

where the Lagrange multiplier λ is the negative root of

$$\lambda^2 = \ln(t)\ln\left(\frac{t}{1-t}\right) + \int_t^{1-t} du\frac{\ln(1-u)}{u}. \tag{27}$$

At t tends to zero, the shape tends to the square $\max(|x|,|y|) = \sqrt{s}/2$. When t tends to $1/2$, then λ tends to zero and the shape tends to $|x| + |y| = \sqrt{s/2}$. When $t = 1$, The shape Eq. (26) reduces to that for unrestricted partitions [22, 23].

The term in the exponential of Eq. (19) can be calculated by substituting Eqs. (25), (26) and (27) into Eq. (24). Doing so, we obtain

$$C_s(t) \sim \frac{1}{s^{1/4}} e^{\lambda\sqrt{s}}, \tag{28}$$

where λ is a function of t determined by Eq. (27). The equilibrium shape of a convex polygon enclosing an area 10000 when $t = 0.15$ is shown in Fig. 3. The four staircase paths intersect each other at a finite angle. The reason why we see cusps in the macroscopic shape is the term proportional to $|y'|\ln(|y'|)$ in the expression for the direction dependent surface tension $\sigma(y')$. This singular term makes $\sigma(y')$ a local maximum at $y' = 0$, which leads to a cusp. The macroscopic shape has four cusps due to the four-fold symmetry of the square lattice.

A similar analysis can be done for convex polygons on a hexagonal lattice. The surface energy $\sigma(y')$ has qualitatively the same behavior as for the square lattice. The six fold symmetry of the hexagonal lattice results in 6 cusps for the hexagonal convex polygons.

For ordinary percolation, the continuum theory calculation [13] gives $\theta_{perc} = 5/4$. On the other hand, θ_{conv} for

a n-sided convex polygon takes on the value $5/4-n/4$. In addition, the macroscopic shape of a n-sided convex polygon has n cusps. These cusps are not expected to appear in the macroscopic shape of percolation clusters. One would presume that on going beyond the convex polygons approximation, these cusps would disappear, each contributing a certain factor to the power law. Thus, putting $n = 0$ in Eq. (21), we recover the result for percolation.

We can similarly determine the value of $\theta_{dir\ perc}$ for two dimensional directed percolation (see [24] for definition and an introduction). Consider directed percolation above the percolation threshold. Let the infinite cluster have a finite opening angle $\pi/2 - 2\gamma$, where γ is a function of p. Then, the surface tension for surfaces which have slopes $\tan(\gamma)$ and $\tan(3\pi/2 - \gamma)$ is zero. Due to these local minima, and hence a maximum at zero slope, the macroscopic shape of finite directed percolation has a cusp at the origin with an opening angle $\pi/2-2\gamma$. Thus, $\theta_{dir\ perc}$ for directed percolation is obtained by substituting $n = 1$ in Eq. (21), yielding

$$\theta_{dir\ perc} = 1 \quad \text{in 2-dimensions.} \tag{29}$$

IV. SUB-CLASSES OF CONVEX POLYGONS

In this section, we extend the results to sub-classes of convex polygons. A directed convex polygon on a square lattice is a convex polygon for which the lower left corner of the bounding rectangle is also a vertex of the polygon (see Fig. 4(a)). As for convex polygons, the area and perimeter weighted generating function for directed convex polygons is known [15, 16]. We now determine the exponent θ in exactly the same way as was done for convex polygons.

Consider a directed convex polygon. The contribution to the power law prefactor from the various steps in the power counting is as follows. (1) The integrand initially has a power law factor $(\sqrt{s})^8$. (2) Integration over x_1, y_1, x_3, y_3 contributes $s^{-1/2}$ each to the power law factor. (3) Integration over x_2, y_2, l, m contributes $s^{-1/4}$ each to the power law factor. (4) Integration over N_1, N_2, N_3 contributes $(s^{-1/4})^2 s^{-1}$ to the power law factor. Collecting together the various terms, we obtain

$$\theta_{dir\ conv} = \frac{1}{2}, \tag{30}$$

where $\theta_{dir\ conv}$ is the θ corresponding to directed convex polygons. The macroscopic shape of the directed convex polygon has three cusps. Not surprisingly, substituting $n = 3$ in Eq. (21) gives the result in Eq. (30).

The other sub-classes of convex polygons that we study are staircase polygons, pyramidal polygons and Ferrers diagrams. Staircase polygons are convex polygons for which both the lower left and upper right corners of the bounding rectangle are vertices of the polygon. Pyramidal polygons are convex polygons for which both the lower left and lower right corners of the bounding rectangle are vertices of the polygon. Ferrers diagrams are convex polygons for which the lower left, lower right and upper left corners of the bounding rectangle are vertices of the polygons. Examples of the polygons are shown in Fig. 4(b), 4(c) and 4(d) respectively. The area and perimeter generating function of staircase polygons [25, 26], pyramidal polygons [22] and Ferrers diagram [18] are known. The exponent θ can be calculated for each one of them as before. Proceeding on the same lines, we obtain

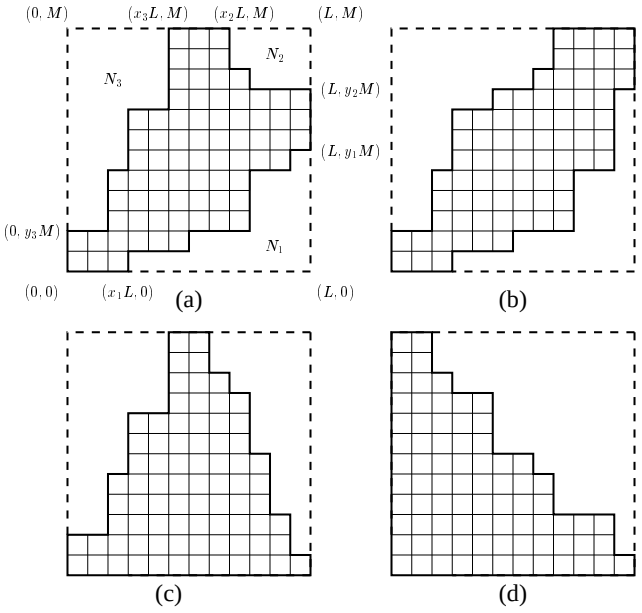

FIG. 4: Examples of (a) a directed convex polygon, (b) a staircase polygon, (c) a pyramidal polygon and (d) Ferrers diagram on a square lattice.

$$\theta_{stair} = \frac{3}{4}, \tag{31}$$

$$\theta_{pyramid} = \frac{1}{2}, \tag{32}$$

$$\theta_{Ferrer} = \frac{1}{2}. \tag{33}$$

These correspond to 2, 3 and 3 cusps respectively in the macroscopic equilibrium shape of these polygons.

V. COLUMN CONVEX POLYGONS

In this section, we determine the equilibrium shape of column-convex polygons and show that it has two cusps. An example of a column-convex polygon is shown in Fig. 5(a). The area and perimeter weighted generating function for column-convex polygons is known [26]. However, as for convex polygons, it is difficult to extract from it the asymptotic behavior of fixed area polygons.

We first calculate the angle dependent surface tension $\sigma_r(\gamma)$, where $y' = \tan(\gamma)$, for column-convex polygons.

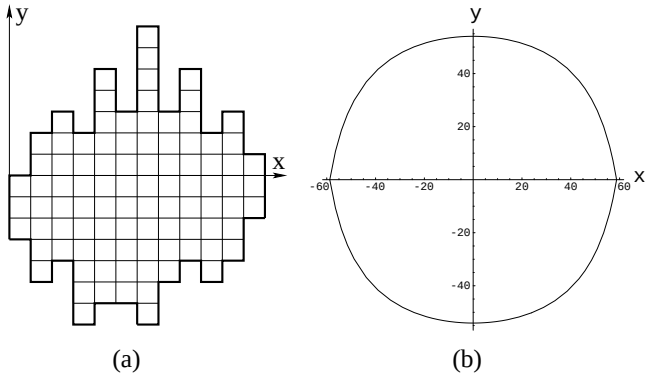

FIG. 5: (a) A column-convex polygon on a square lattice. Any line in the vertical direction intersects the polygon at either zero or two points. (b) The equilibrium macroscopic shape of a column-convex polygon on a square lattice enclosing an area 10000, when $t = 0.15$.

This analysis is similar to that done for directed polymers [27]. Consider all possible directed walks from $(0, 0)$ to (x, y). Then, the sum over all weighted paths is

$$e^{-x\sec(\gamma)\sigma_r(\gamma)} = \sum_{y_1,\ldots,y_x} \delta\left(\sum_{i=1}^{x} y_i - y\right) \prod_{i=1}^{x} t^{1+|y_i|}, \quad (34)$$

where δ is the usual Kronecker delta function. Taking Laplace transform with respect to y, we obtain independent summations over y_i. These are easily done giving

$$\sigma_r(y')\sqrt{1+y'^2} = y'\ln(z_0) + \ln\frac{(1-tz_0)(1-tz_0^{-1})}{t(1-t^2)}, \quad (35)$$

where

$$z_0 = \frac{(1+t^2)y' + \sqrt{(1-t^2)^2y'^2 + 4t^2}}{2t(1+y')}. \quad (36)$$

We see that $\sigma_r(y')$ is now a smooth function of y' for y' near zero. For convex polygons, a surface with average orientation $y' = 0$ cannot have any fluctuations, as the height fluctuations in the y-direction become the disallowed overhangs in the x-direction. This leads to the singularity near $y' = 0$ in the expression for orientation dependent surface tension for convex polygons.

To construct the equilibrium shape of the polygon, we need to find the $y(x)$ satisfying the Euler Lagrange equation (see Eq. (24)) with σ_r and a Lagrange multiplier λ_r. The curve $y(x)$ satisfies the boundary condition $y(-X/2) = 0$ and $y(X/2) = 0$. Solving, we find that the shape of the polygon is given by

$$e^{2\lambda_r y/\sqrt{s}} = 4ct\sinh\left(\frac{\ln(t)}{2} - \frac{\lambda_r x}{\sqrt{s}}\right)\sinh\left(\frac{\ln(t)}{2} + \frac{\lambda_r x}{\sqrt{s}}\right), \quad (37)$$

where c is a constant, $X = g(c)\sqrt{s}/\lambda_r$ and

$$g(c) = \ln\left[\frac{c(1+t^2) - 1 + \sqrt{(1-c(1-t^2))^2 - 4c^2t^2}}{2ct}\right]. \quad (38)$$

The Lagrange multiplier λ_r is fixed by the constraint that $\int_{-X/2}^{X/2} y dx = s/2$. We obtain λ_r as a function of c to be

$$\lambda_r^2 = \int_0^{g(c)} dz \ln\left[c(1-te^{-z})(1-te^{z})\right]. \quad (39)$$

The value of c is chosen to be the one that minimizes the total surface free energy. For the curve Eq. (37), the total surface energy $F(c, t)$ is

$$F(c,t) = 2\lambda_r\sqrt{s} - \frac{\sqrt{s}}{\lambda_r}g(c)\ln\left[ct(1-t^2)\right]. \quad (40)$$

Minimizing Eq. (40) with respect to c, we obtain

$$c = \frac{1}{t(1-t^2)}. \quad (41)$$

Equations (37), (39) and (41) describe the equilibrium shape of column-convex polygons. In Fig. 5(b), the shape when $t = 0.15$ is shown. It has two cusps. Thus, we would conclude from Eq. (21) that

$$\theta_{col\ conv} = \frac{3}{4}. \quad (42)$$

The height fluctuations of the column-convex polygons become overhangs when viewed after rotation by $\pi/2$. On introducing such overhangs, two of the four cusps that were present in the shape of convex polygons vanished. Thus, one would expect that if overhangs in the horizontal direction were also allowed as in self avoiding polygons, then there would be no cusps, and

$$\theta_{poly} = \frac{5}{4}. \quad (43)$$

Finally, we note that the macroscopic shape of column-convex polygons becomes unstable when $\sigma_r(0) = 0$. The smallest absolute value of t at which this occurs is

$$t_c = \sqrt{2} - 1. \quad (44)$$

This value matches with the previously obtained value for t_c [28, 29].

VI. SUMMARY AND CONCLUSION

To summarize, we studied fixed area convex polygons weighted by their perimeter on square and hexagonal lattices. The exponent θ_{conv} as defined in Eq. (2) was found to be $1/4$ for the square lattice and $-1/4$ for the hexagonal lattice. This discrepancy was traced to the presence of cusps in the macroscopic shape of convex polygons. We argued that for a polygon whose macroscopic shape has n cusps has $\theta_n = (5-n)/4$. For polygons, one expects that the macroscopic shape has no cusps. Indeed, putting $n = 0$ in Eq. (21), we recover the result $\theta_{perc} = 5/4$ obtained for percolation clusters [13]. For directed percolation, it is argued that there should be one cusp, and hence $\theta_{dir\ perc} = 1$ in two dimensions.

Acknowledgments

R. Rajesh would like to acknowledge EPSRC, U.K. for financial support.

---

[1] E. J. J. van Rensburg, *The Statistical Mechanics of Interacting Walks, Polygons, Animals and Vesicles* (Oxford University Press, Oxford, 2000).
[2] S. Leibler, R. R. P. Singh and M. E. Fisher, Phys. Rev. Lett. **59**, 1989 (1987)
[3] M. E. Fisher, A. J. Guttmann and S. G. Whittington, J. Phys. A **24**, 3095 (1991).
[4] M. Bousquet-Mélou, Disc. Math. **154**, 1 (1996).
[5] Articles by A. J. Guttmann and K. Y. Lin in *Computer-Aided Statistical Physics*, AIP Conference Proceedings **248**, edited by C. -K. Hu.
[6] C. Richard, A. J. Guttmann and I. Jensen, J. Phys. A **34**, L495 (2001).
[7] J. Cardy, J. Phys. A **34**, L665 (2001).
[8] C. Richard, J. Stat. Phys. **108**, 459 (2002).
[9] C. Richard, I. Jensen and A. J. Guttmann, cond-mat/0302513.
[10] D. Stauffer and A. Aharony, *Introduction to Percolation Theory* (Taylor and Francis, London, 1994).
[11] D. Stauffer, Phys. Rep. **54**, 1 (1979).
[12] H. Kunz and B. Souillard, Phys. Rev. Lett. **40**, 133 (1978); J. Stat. Phys. **19**, 77 (1978).
[13] T. C. Lubensky and A. J. McKane, J. Phys. A **14**, L157 (1981).
[14] K. Y. Lin, J. Phys. A **24**, 2411 (1991).
[15] M. Bousquet-Mélou, J. Phys. A **25**, 1925 (1992).
[16] M. Bousquet-Mélou, J. Phys. A **25**, 1935 (1992).
[17] T. Prellberg and A. L. Owczarek, Commun. Math. Phys. **201**, 493 (1999).
[18] G. E. Andrews, *The Theory of Partitions*, Encyclopedia of Mathematics and its Applications Vol **2**, (Addison-Wesley, Reading, 1976).
[19] Chapter 6 in C. M. Bender and S. A. Orszag, *Advanced Mathematical Methods for Scientists and Engineers* (McGraw-Hill, New York, 1978).
[20] G. H. Hardy and S. Ramanujan, Proc. London Math. Soc. **17**, 75 (1918).
[21] C. Rottman and M. Wortis, Phys. Rep. **103**, 59 (1984).
[22] H. N. V. Temperley, Proc. Camb. Phi. Soc. **48**, 683 (1952).
[23] -A. -M. Vershik, Funct. Anal. Appl. **30**, 90 (1996).
[24] H. Hinrichsen, Adv. Phys. **49**, 815 (2000).
[25] G. Pólya, J. Combin. Theor. **6**, 102 (1969).
[26] R. Brak and A. J. Guttmann, J. Phys. A **23**, 4581 (1990).
[27] R. Rajesh, D. Dhar, D. Giri, S. Kumar and Y. Singh, Phys. Rev. E, **65**, 056124 (2002).
[28] H. N. V. Temperley, Phys. Rev. **103**, 1 (1956).
[29] R. Brak, A. J. Guttmann and I. G. Enting, J. Phys. A **23**, 2319 (1990).